Acta Cryst E CRYSTALLOGRAPHIC COMMUNICATIONS
ISSN 2056-9890

Crystal structure and photoluminescent properties of a new Eu^{III}–phthalate–acetate coordination polymer

Prakottakarn Jittipiboonwat,[a] Thammanoon Chuasaard[a] and Apinpus Rujiwatra[a,b]*

[a]Department of Chemistry, Faculty of Science, Chiang Mai University, Chiang Mai, 50200, Thailand, and [b]Materials Science Research Center, Faculty of Science, Chiang Mai University, Chiang Mai 50200, Thailand. *Correspondence e-mail: apinpus.rujiwatra@cmu.ac.th

Received 8 April 2022
Accepted 22 April 2022

Edited by A. Briceno, Venezuelan Institute of Scientific Research, Venezuela

Keywords: coordination polymer; lanthanide; phthalate; acetate; crystal structure; photoluminescence.

CCDC reference: 2168116

Supporting information: this article has supporting information at journals.iucr.org/e

A new coordination polymer, poly[(acetato)aqua(μ_3-phthalato)europium(III)], $[Eu(C_8H_4O_4)(CH_3O_2)(H_2O)]_n$ or $[Eu^{III}(phth)(OAc)(H_2O)]$ ($phth^{2-}$ = phthalate and OAc^- = acetate) was synthesized and characterized, revealing it to be a supramolecular assembly of one-dimensional $[Eu^{III}(phth)(OAc)(H_2O)]$ chains. Each chain is built up of edge-sharing distorted tricapped trigonal–prismatic *TPRS*-$\{Eu^{III}O_9\}$ building motifs and assembled in a regular fashion through hydrogen-bonding and aromatic π–π interactions. The fully deprotonated $phth^{2-}$ ligand was shown to be an effective sensitizer, promoting the characteristic $^5D_0 \rightarrow {}^7F_J$ (J = 1–4) emissions of Eu^{III} even in the presence of the non-sensitizing OAc^- group.

1. Chemical context

Interest in crystal engineering of lanthanide coordination polymers has been driven by the unique coordination chemistry and electronic properties of trivalent lanthanides (Ln^{III}), which bring about a wide variety of potential applications ranging from, for instance, luminescence sensing (Hasegawa & Kitagawa, 2022), magnetism (Hu *et al.*, 2021), catalysis (Sinchow *et al.*, 2021), gas storage and separation (Li & Chen, 2014), to drug delivery (Wei *et al.*, 2020) and biomolecular imaging (Miller *et al.*, 2016). However, the high coordination numbers, flexible coordination geometries and lack of directionality of Ln—O bonds complicate prediction of the designed polymeric frameworks, which are also greatly influenced by differences in synthetic parameters, *i.e.* reaction temperature and time, solvent, pH of reaction, *etc* (Bünzli, 2014; Qiu & Zhu, 2009). The study of structure–property relationships, which is an essence of property design, is consequently limited.

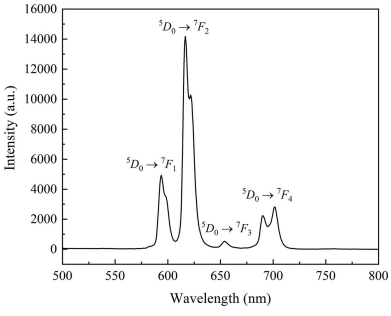

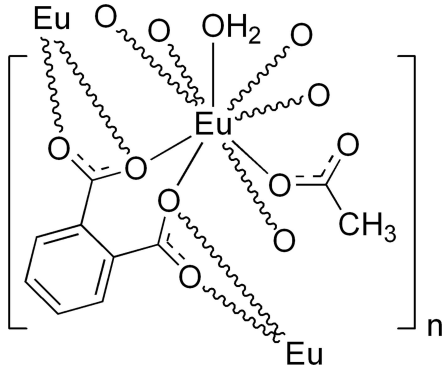

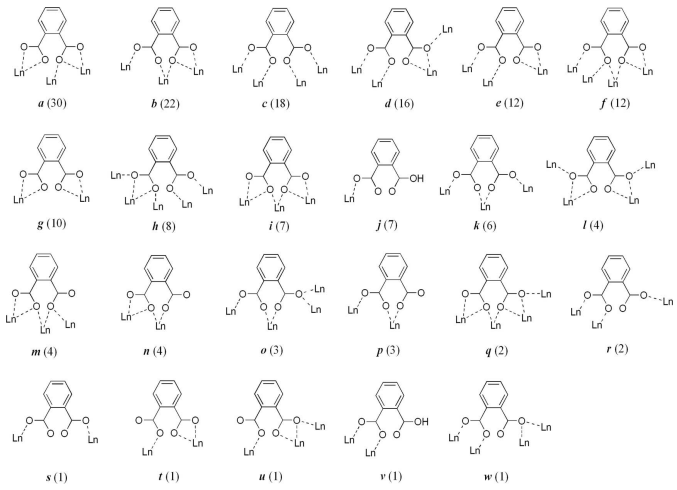

Figure 1
Coordination modes of $phth^{2-}$ and $Hphth^{-}$ found in lanthanide coordination compounds deposited to the CSD (Groom *et al.*, 2016) with frequency of appearance in parentheses.

Unlike transition-metal-based coordination polymers in which the preferred coordination geometries of the transition-metal ions play an important role in directing the framework architecture (Kitagawa *et al.*, 2004), those based on Ln^{III} are principally governed by the organic ligands. Polycarboxylic acids are notably the most commonly utilized, facilitating diversity through their modes of coordination such as those found for phthalic acid (H_2phth) (Fig. 1). These coordination modes can also be diversified through the presence of the other ligands such as those found in, for instance, $[Ln^{III}(bdc)_{0.5}(phth)(H_2O)_2]$ (Ln^{III} = Eu^{III}, Tb^{III}, Ho^{III}, Er^{III} and Tm^{III}, H_2bdc = terephthalic acid; Chuasaard *et al.*, 2020), $[Ln^{III}(abdc)_{0.5}(phth)(H_2O)_2]\cdot 2H_2O$ (Ln^{III} = Eu^{III}, Gd^{III} and Tb^{III}, H_2abdc = azobenzene-4,4′-dicarboxylic acid; Chuasaard *et al.*, 2022) and $[Ln^{III}(ox)(phth)(H_2O)_2]\cdot 0.5H_2O$ (Ln^{III} = Sm^{III} and Tb^{III}, H_2ox = oxalic acid; Wang *et al.*, 2010).

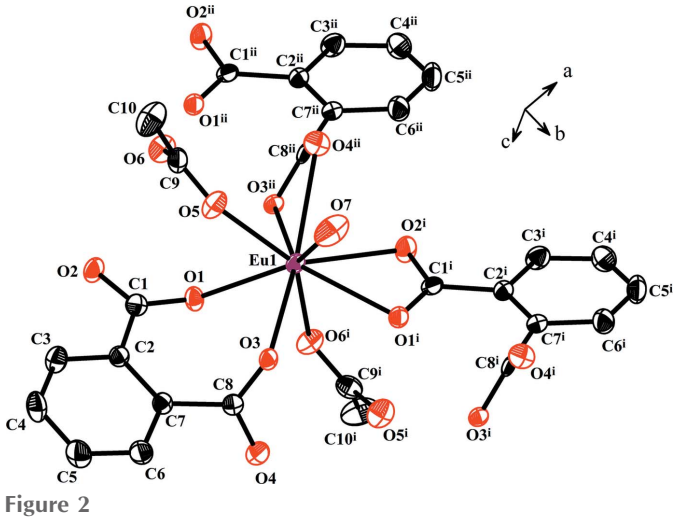

Figure 2
Extended asymmetric unit of the title compound drawn using 50% probability for ellipsoids (hydrogen atoms are omitted for clarity). Symmetry codes: (i) $\frac{3}{2}-x, \frac{1}{2}+y, \frac{3}{2}-z$; (ii) $\frac{3}{2}-x, -\frac{1}{2}+y, \frac{3}{2}-z$.

Table 1
Selected bond lengths (Å).

Eu1—O1^{i}	2.570 (2)	Eu1—O4^{ii}	2.605 (2)
Eu1—O1	2.397 (2)	Eu1—O5	2.352 (2)
Eu1—O2^{i}	2.474 (2)	Eu1—O6^{i}	2.434 (3)
Eu1—O3	2.381 (2)	Eu1—O7	2.446 (2)
Eu1—O3^{ii}	2.484 (2)		

Symmetry codes: (i) $-x+\frac{3}{2}, y+\frac{1}{2}, -z+\frac{3}{2}$; (ii) $-x+\frac{3}{2}, y-\frac{1}{2}, -z+\frac{3}{2}$.

With respect to photoluminescence, $phth^{2-}$ is acknowledged as a good sensitizer and can effectively promote *f*–*f* emissions in, for example, $[Eu^{III}_2(phth)_3(H_2O)]$ (Wan *et al.*, 2002). The apparent photoluminescence can, nonetheless, be modulated by the other ligands such as ad^{2-} in $[Ln^{III}(ad)_{0.5}(phth)(H_2O)_2]$ (Chuasaard *et al.*, 2018) and bdc^{2-} in $[Ln^{III}(bdc)_{0.5}(phth)(H_2O)_2]$ (Chuasaard *et al.*, 2020).

2. Structural commentary

The asymmetric unit of the title compound, $[Eu^{III}(phth)(OAc)(H_2O)]$, is composed of one crystallographically unique Eu^{III} ion, a whole molecule of $phth^{2-}$, and the coordinating OAc^{-} and water molecules (Fig. 2). The Eu^{III} ion is ninefold coordinated to O atoms from three $phth^{2-}$, two OAc^{-} and one water molecule, which define a distorted tricapped trigonal–prismatic *TPRS*-$\{Eu^{III}O_9\}$ building motif. The Eu—O bond distances are in the range 2.352 (2)-2.605 (2) Å (Table 1), which are consistent with those reported for other Eu^{III} frameworks of $phth^{2-}$ and OAc^{-}, *viz.* $[Eu^{III}(abdc)_{0.5}(phth)(H_2O)_2]\cdot 2H_2O$ (Chuasaard *et al.*, 2022), $[Eu^{III}(phth)(STP)]$ (NaSTP = sodium 2-(2,2′:6′,2″-terpyridin-4′-yl)benzenesulfonate; Hu *et al.*, 2019) and $[C_2mim]_2[Eu_2(OAc)_8]$ (C_2mim = 1-ethyl-3-methylimidazolium; Bousrez *et al.*, 2021). The *TPRS*-$\{Eu^{III}O_9\}$ motifs are fused through the μ_2-O atoms of $phth^{2-}$, forming an infinite one-dimensional zigzag chain of edge-sharing *TPRS*-$\{Eu^{III}O_9\}$ motifs extending

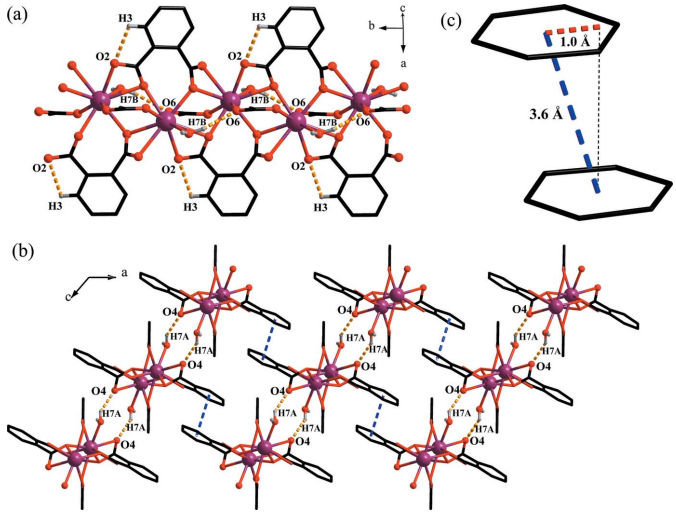

Figure 3
Depiction of (*a*) intrachain and (*b*) interchain hydrogen-bonding interactions, and (*c*) π–π interactions.

Table 2
Hydrogen-bond geometry (Å, °).

D—H···A	D—H	H···A	D···A	D—H···A
O7—H7A···O4^{iii}	0.85	2.17	2.9384	149
O7—H7B···O6^{iv}	0.85	2.28	3.0438	150
C3—H3···O2	0.93	2.46	2.7741	100

Symmetry codes: (iii) $x, -y, z-\frac{1}{2}$; (iv) $-x+\frac{1}{2}, y+\frac{1}{2}, -z+\frac{1}{2}$.

along the *b*-axis direction. Not only phth^{2-}, which helps facilitating the formation of the one-dimensional chain through the overall μ_3-η^1:η^2:η^2:η^1 mode of coordination (mode *i* in Fig. 1), but also the smaller OAc$^-$ link adjacent Eu^{III} centers in a bridging μ_2-η^1:η^1 coordination mode.

3. Supramolecular features

The three-dimensional supramolecular assembly of [Eu^{III}(phth)(OAc)(H$_2$O)] chains are facilitated by hydrogen bonding and aromatic π–π interactions (Fig. 3). The hydrogen-bonding interactions can be divided into the interchain O7—H7A···O4 and the intrachain O7—H7B···O6 and C3—H3···O2 interactions (Table 2). The π–π interaction between neighboring chains is considered to be of the displaced-stacking type (Banerjee *et al.*, 2019; Yao *et al.*, 2018), with an interplanar angle of 0°, an offset distance of *ca* 1.0 Å and a centroid-to-centroid distance of *ca* 3.6 Å.

4. Photoluminescent properties

The emission spectrum of ground crystals of the title compound was recorded at room temperature. Upon the excitation at 370 nm, the characteristic red emission originating from the $^5D_0\rightarrow{}^7F_J$ (J = 1–4) transitions of Eu^{III} were displayed (Fig. 4). This indicates the efficiency of phth^{2-} as a good sensitizer, even in the presence of the non-sensitizing

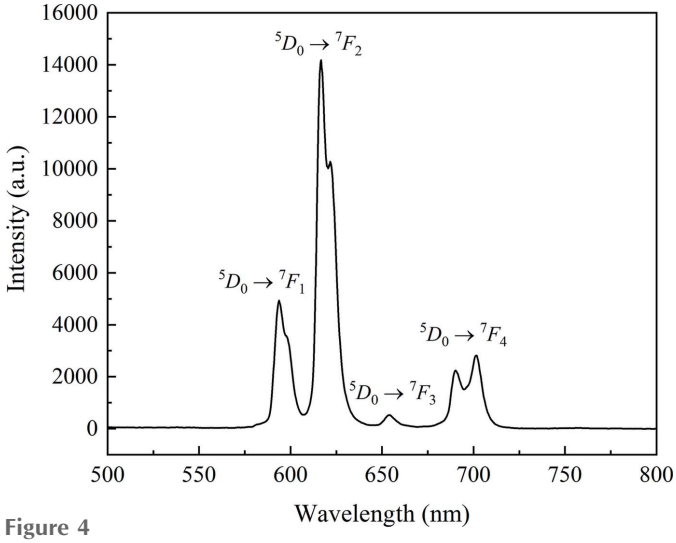

Figure 4
Room-temperature photoluminescent emission spectrum of the title compound.

OAc$^-$. A split of the very intense $^5D_0\rightarrow{}^7F_2$ emission suggests that the Eu^{III} ion is not located at a site with a center of symmetry (Binnemans, 2015), which is consistent with its distorted tricapped trigonal–prismatic coordination geometry. The split of the $^5D_0\rightarrow{}^7F_4$ emission, on the other hand, should be due to the ligand-field effect (Gupta *et al.*, 2015; Okayasu & Yuasa, 2021; Puntus *et al.*, 2010).

5. Database survey

A search of the CSD database (CSD version 5.43, update of November 2021; Groom *et al.*, 2016) using the ConQuest software (version 2021.3.0; Bruno *et al.*, 2002), found 115 structures of lanthanide compounds including phth^{2-}. In six of these structures, phth^{2-} adopts the same μ_3-η^1:η^2:η^2:η^1 mode of coordination as in the title compound. This mode of coordination apparently promotes the formation of a one-dimensional coordination framework, as, for example, in [Pr$_3$(phen)$_2$(phth)$_4$(NO$_3$)]·H$_2$O (phen = 1,10-phenanthroline) (refcode: LAXWOX; Thirumurugan & Natarajan, 2005), [Nd(Nphgly)(phth)(H$_2$O)]·2H$_2$O (Nphgly = *N*-phthaloylglycine) (refcode: TOHJEH; Yang *et al.*, 2014), and [Gd$_2$Ni(2,5-pdc)$_2$(phth)$_2$(H$_2$O)$_4$]·8H$_2$O (2,5-H$_2$pdc = 2,5-pyridinedicarboxylic acid) (refcode: XOZYER; Mahata *et al.*, 2009).

Regarding OAc$^-$, there are 566 structures containing this deposited in the CSD, none of which also contains phth^{2-}. There are, however, structures containing both OAc$^-$ and isophthalate (iso-phth^{2-}), *e.g.* [Sm$_2$(iso-phth)$_2$(OAc)$_2$-(H$_2$O)$_4$]·H$_2$O (refcode: VOJNAK; Jin *et al.*, 2008), and [Dy$_4$(iso-phth)$_4$(OAc)$_4$(H$_2$O)$_8$]·2H$_2$O (refcode: DIBZEU; Hu *et al.*, 2007).

6. Synthesis and crystallization

All chemicals used in this work were obtained commercially and used without purification: Eu$_2$O$_3$ (Strategic Elements, 99.99%), phthalic acid (H$_2$phth; C$_8$H$_6$O$_4$, BDH laboratory, 99%), NaOH (RCI Labscan, 99.0%), glacial acetic acid (AcOH; CH$_3$COOH, QRëC, 99.8%), tetrahydrofuran (THF; C$_4$H$_8$O, RCI Labscan, 99.8%), ethanol (EtOH; C$_2$H$_5$OH, RCI Labscan, 99.7%). Eu(OAc)$_3$·4H$_2$O, was prepared by dissolving Eu$_2$O$_3$ (2.5000 g, 7.1038 mmol) in 50.0 mL of deionized water with a few drops of glacial acetic acid (HOAc). After the pH of the suspension was adjusted to 3 using HOAc, the mixture was gently heated and a colorless homogeneous solution was attained. The white powder of Eu(OAc)$_3$·4H$_2$O was then recovered through slow evaporation of the solvent.

To synthesize the title compound, Eu(OAc)$_3$·4H$_2$O (0.16 g, 0.40 mmol) was dissolved in 2.0 mL of deionized water to prepare solution **A**. Solution **B** was separately prepared by dissolving Na$_2$phth (84 mg, 0.40 mmol) and NaOAc (33 mg, 0.4 mmol) in a mixed solvent prepared from 1.0 mL of deionized water and 5.0 mL of tetrahydrofuran (THF). Solutions **A** and **B** were then mixed in a 15 mL glass vial. The volume of the reaction was adjusted to 10.0 mL using deionized water and the pH of the solution was adjusted to 4 using HOAc. The reaction was left under stirring at room temperature for 2 h,

Table 3
Experimental details.

Crystal data	
Chemical formula	$[Eu(C_8H_4O_4)(CH_3O_2)(H_2O)]$
M_r	393.13
Crystal system, space group	Monoclinic, *C*2/*c*
Temperature (K)	293
a, *b*, *c* (Å)	26.5184 (15), 7.2632 (2), 15.3622 (8)
β (°)	130.906 (9)
V (Å^3)	2236.3 (3)
Z	8
Radiation type	Mo $K\alpha$
μ (mm^{-1})	5.63
Crystal size (mm)	0.2 × 0.1 × 0.1
Data collection	
Diffractometer	Rigaku SuperNova, single source at offset/far, HyPix3000
Absorption correction	Multi-scan (*CrysAlis PRO*; Rigaku OD, 2019)
T_{min}, T_{max}	0.218, 1.000
No. of measured, independent and observed [$I > 2\sigma(I)$] reflections	9923, 2393, 2138
R_{int}	0.032
(sin $\theta/\lambda)_{max}$ (Å^{-1})	0.648
Refinement	
$R[F^2 > 2\sigma(F^2)]$, $wR(F^2)$, S	0.024, 0.052, 1.05
No. of reflections	2393
No. of parameters	167
No. of restraints	1
H-atom treatment	H-atom parameters constrained
$\Delta\rho_{max}$, $\Delta\rho_{min}$ (e Å^{-3})	0.64, −0.79

Computer programs: *CrysAlis PRO* (Rigaku OD, 2019), *SHELXT2018/2* (Sheldrick, 2015*a*), *SHELXL2018/3* (Sheldrick, 2015*b*) and *OLEX2* (Dolomanov *et al.*, 2009).

after which the solvent was slowly evaporated, leading to the crystallization of colorless block-shaped crystals of [Eu(phth)(OAc)(H_2O)] (78% yield based on Eu^{III}). The crystals were characterized using FT–IR spectroscopy (PerkinElmer/Frontier FT–IR instrument; ATR mode; cm^{-1}): 3541(*br*), 3419(*br*), 2978(*w*), 1548(*w*), 1402(*m*), 1373(*m*), 804(*s*), 754(*s*), 707(*s*), 650(*s*), 543(*m*), 503(*m*). The room-temperature photoluminescent spectrum was collected using a ASEQ LR-1T broad-range spectrophotometer equipped with an Ultrafire G60 UV LED Flashlight Torch excitation source (5 W, 370 nm)

7. Refinement

Crystal data, data collection and structure refinement details are summarized in Table 3. All H atoms were positioned geometrically and refined isotropically using a riding model. The C—H bond lengths in the aromatic phth^{2-} linker and in OAc$^-$ were restrained to 0.93 Å [U_{iso}(H) = 1.2U_{eq}(C)] and 0.96 Å [U_{iso}(H) = 1.5U_{eq}(C)], respectively. The O—H bond lengths in the coordinated water molecule were restrained to 0.85 Å with U_{iso}(H) = 1.5U_{eq}(O).

Funding information

This research was funded by Chiang Mai University and the Program Management Unit – Brain Power (PMU B), The Office of National Higher Education Science Research and Innovation Policy Council (NXPO) in a Global Partnership Project.

References

Banerjee, A., Saha, A. & Saha, B. K. (2019). *Cryst. Growth Des.* **19**, 2245–2252.
Binnemans, K. (2015). *Coord. Chem. Rev.* **295**, 1–45.
Bousrez, G., Renier, O., Kelley, S. P., Adranno, B., Tahavori, E., Titi, H. M., Smetana, V., Tang, S.-F., Mudring, A.-V. & Rogers, R. D. (2021). *Chem. Eur. J.* **27**, 13181–13189.
Bruno, I. J., Cole, J. C., Edgington, P. R., Kessler, M., Macrae, C. F., McCabe, P., Pearson, J. & Taylor, R. (2002). *Acta Cryst.* B**58**, 389–397.
Bünzli, J.-C. G. (2014). *J. Coord. Chem.* **67**, 3706–3733.
Chuasaard, T., Ngamjarurojana, A., Konno, T. & Rujiwatra, A. (2020). *J. Coord. Chem.* **73**, 333–345.
Chuasaard, T., Ngamjarurojana, A., Surinwong, S., Konno, T., Bureekaew, S. & Rujiwatra, A. (2018). *Inorg. Chem.* **57**, 2620–2630.
Chuasaard, T., Thammakan, S., Semakul, N., Konno, T. & Rujiwatra, A. (2022). *J. Mol. Struct.* **1251**, 131940.
Dolomanov, O. V., Bourhis, L. J., Gildea, R. J., Howard, J. A. K. & Puschmann, H. (2009). *J. Appl. Cryst.* **42**, 339–341.
Groom, C. R., Bruno, I. J., Lightfoot, M. P. & Ward, S. C. (2016). *Acta Cryst.* B**72**, 171–179.
Gupta, S. K., Ghosh, P. S., Sahu, M., Bhattacharyya, K., Tewari, R. & Natarajan, V. (2015). *RSC Adv.* **5**, 58832–58842.
Hasegawa, Y. & Kitagawa, Y. (2022). *J. Photochem. Photobiol. Photochem. Rev.* **51**, 100485.
Hu, D.-X., Chen, P.-K., Luo, F., Che, Y.-X. & Zheng, J.-M. (2007). *J. Mol. Struct.* **837**, 179–184.
Hu, J.-J., Peng, Y., Liu, S.-J. & Wen, H.-R. (2021). *Dalton Trans.* **50**, 15473–15487.
Hu, Y.-C., Bai, C., Hu, H.-M., Li, C.-T., Zhang, T.-H. & Liu, W. (2019). *Acta Cryst.* B**75**, 855–864.
Jin, Y., Luo, F., Che, Y.-X. & Zheng, J. M. (2008). *Inorg. Chem. Commun.* **11**, 711–713.
Kitagawa, S., Kitaura, R. & Noro, S.-I. (2004). *Angew. Chem. Int. Ed.* **43**, 2334–2375.
Li, B. & Chen, B. (2014). *Lanthanide Metal–Organic Frameworks. Structure and Bonding*, edited by P. Cheng, pp. 75–107. Berlin, Heidelberg: Springer.
Mahata, P., Ramya, K. V. & Natarajan, S. (2009). *Inorg. Chem.* **48**, 4942–4951.
Miller, S. E., Teplensky, M. H., Moghadam, P. Z. & Fairen-Jimenez, D. (2016). *Interface Focus*, **6**, 20160027.
Okayasu, Y. & Yuasa, J. (2021). *J. Phys. Chem. Lett.* **12**, 6867–6874.
Puntus, L. N., Lyssenko, K. A., Pekareva, I. S. & Antipin, M. Y. (2010). *Mol. Phys.* **108**, 557–572.
Qiu, S. & Zhu, G. (2009). *Coord. Chem. Rev.* **253**, 2891–2911.
Rigaku OD (2019). *CrysAlis PRO*. Rigaku Oxford Diffraction, Yarnton, England.
Sheldrick, G. M. (2015*a*). *Acta Cryst.* A**71**, 3–8.
Sheldrick, G. M. (2015*b*). *Acta Cryst.* C**71**, 3–8.
Sinchow, M., Semakul, N., Konno, T. & Rujiwatra, A. (2021). *ACS Sustainable Chem. Eng.* **9**, 8581–8591.
Thirumurugan, A. & Natarajan, S. (2005). *J. Mater. Chem.* **15**, 4588–4594.
Wan, Y., Jin, L., Wang, K., Zhang, L., Zheng, X. & Lu, S. (2002). *New J. Chem.* **26**, 1590–1596.
Wang, Z., Xing, Y.-H., Wang, C.-G., Sun, L.-X., Zhang, J., Ge, M.-F. & Niu, S.-Y. (2010). *CrystEngComm*, **12**, 762–773.
Wei, D., Xin, Y., Rong, Y., Li, Y., Zhang, C., Chen, Q., Qin, S., Wang, W. & Hao, Y. (2020). *J. Inorg. Organomet. Polym.* **30**, 1121–1131.
Yang, Y.-T., Tu, C.-Z., Yin, H.-J. & Cheng, F.-X. (2014). *Inorg. Chem. Commun.* **46**, 107–109.
Yao, Z.-F., Wang, J.-Y. & Pei, J. (2018). *Cryst. Growth Des.* **18**, 7–15.

supporting information

Acta Cryst. (2022). E**78**, 536-539 [https://doi.org/10.1107/S2056989022004339]

Crystal structure and photoluminescent properties of a new Eu^{III}–phthalate–acetate coordination polymer

Prakottakarn Jittipiboonwat, Thammanoon Chuasaard and Apinpus Rujiwatra

Computing details

Data collection: *CrysAlis PRO* (Rigaku OD, 2019); cell refinement: *CrysAlis PRO* (Rigaku OD, 2019); data reduction: *CrysAlis PRO* (Rigaku OD, 2019); program(s) used to solve structure: *SHELXT2018/2* (Sheldrick, 2015a); program(s) used to refine structure: *SHELXL2018/3* (Sheldrick, 2015b); molecular graphics: *OLEX2* (Dolomanov *et al.*, 2009); software used to prepare material for publication: *OLEX2* (Dolomanov *et al.*, 2009).

Poly[(acetato)aqua(μ_3-phthalato)europium(III)]

Crystal data

$[Eu(C_8H_4O_4)(CH_3O_2)(H_2O)]$
M_r = 393.13
Monoclinic, *C*2/*c*
a = 26.5184 (15) Å
b = 7.2632 (2) Å
c = 15.3622 (8) Å
β = 130.906 (9)°
V = 2236.3 (3) Å^3
Z = 8
F(000) = 1504
D_x = 2.335 Mg m^{-3}
Mo *Kα* radiation, *λ* = 0.71073 Å
Cell parameters from 7078 reflections
θ = 2.0–27.4°
μ = 5.63 mm^{-1}
T = 293 K
Block, clear light colourless
0.2 × 0.1 × 0.1 mm

Data collection

Rigaku SuperNova, Single source at offset/far, HyPix3000 diffractometer
Radiation source: micro-focus sealed X-ray tube, SuperNova (Mo) X-ray Source
Mirror monochromator
Detector resolution: 10.0000 pixels mm^{-1}
ω scans
Absorption correction: multi-scan (CrysAlisPro; Rigaku OD, 2019)
T_{min} = 0.218, T_{max} = 1.000
9923 measured reflections
2393 independent reflections
2138 reflections with $I > 2\sigma(I)$
R_{int} = 0.032
θ_{max} = 27.4°, θ_{min} = 2.0°
h = −33→33
k = −9→9
l = −19→18

Refinement

Refinement on F^2
Least-squares matrix: full
$R[F^2 > 2\sigma(F^2)]$ = 0.024
$wR(F^2)$ = 0.052
S = 1.05
2393 reflections
167 parameters
1 restraint
Primary atom site location: dual
Hydrogen site location: mixed
H-atom parameters constrained
$w = 1/[\sigma^2(F_o^2) + (0.0235P)^2 + 1.2859P]$ where $P = (F_o^2 + 2F_c^2)/3$
$(\Delta/\sigma)_{max}$ = 0.001
$\Delta\rho_{max}$ = 0.64 e Å^{-3}
$\Delta\rho_{min}$ = −0.79 e Å^{-3}

Special details

Geometry. All esds (except the esd in the dihedral angle between two l.s. planes) are estimated using the full covariance matrix. The cell esds are taken into account individually in the estimation of esds in distances, angles and torsion angles; correlations between esds in cell parameters are only used when they are defined by crystal symmetry. An approximate (isotropic) treatment of cell esds is used for estimating esds involving l.s. planes.

Fractional atomic coordinates and isotropic or equivalent isotropic displacement parameters (Å²)

	x	*y*	*z*	U_{iso}*/U_{eq}
Eu1	0.75770 (2)	0.36927 (2)	0.71208 (2)	0.01709 (7)
O1	0.69745 (10)	0.1993 (3)	0.7522 (2)	0.0219 (5)
O4	0.68510 (12)	0.6542 (3)	0.8366 (2)	0.0264 (6)
O3	0.68174 (10)	0.5756 (3)	0.69468 (19)	0.0185 (5)
O6	0.69030 (12)	−0.0954 (3)	0.5869 (2)	0.0290 (6)
O2	0.62648 (11)	−0.0281 (3)	0.6844 (2)	0.0273 (6)
O7	0.72235 (14)	0.5336 (4)	0.5410 (2)	0.0422 (7)
H7A	0.697069	0.483288	0.474914	0.063*
H7B	0.708422	0.643920	0.528604	0.063*
O5	0.67155 (11)	0.2044 (3)	0.5460 (2)	0.0308 (6)
C7	0.59568 (15)	0.4602 (4)	0.6922 (3)	0.0185 (7)
C2	0.58415 (15)	0.2718 (4)	0.6633 (3)	0.0185 (7)
C8	0.65937 (15)	0.5624 (4)	0.7479 (3)	0.0181 (7)
C9	0.66224 (16)	0.0380 (5)	0.5165 (3)	0.0257 (8)
C1	0.63844 (17)	0.1403 (4)	0.7002 (3)	0.0196 (8)
C10	0.61510 (19)	−0.0007 (5)	0.3902 (3)	0.0412 (10)
H10A	0.616586	−0.129448	0.377789	0.062*
H10B	0.627783	0.070141	0.354452	0.062*
H10C	0.570626	0.032152	0.357152	0.062*
C6	0.54332 (17)	0.5698 (5)	0.6621 (3)	0.0282 (8)
H6	0.551117	0.692945	0.683999	0.034*
C3	0.52024 (16)	0.2027 (5)	0.6028 (3)	0.0257 (8)
H3	0.512351	0.077936	0.585067	0.031*
C4	0.46810 (17)	0.3156 (5)	0.5685 (3)	0.0301 (9)
H4	0.425093	0.268326	0.524046	0.036*
C5	0.47994 (17)	0.4983 (5)	0.6002 (3)	0.0318 (9)
H5	0.445276	0.573408	0.579933	0.038*

Atomic displacement parameters (Å²)

	U^{11}	U^{22}	U^{33}	U^{12}	U^{13}	U^{23}
Eu1	0.01881 (11)	0.01068 (11)	0.02213 (12)	0.00003 (6)	0.01356 (9)	−0.00015 (6)
O1	0.0190 (12)	0.0157 (11)	0.0322 (14)	0.0006 (10)	0.0173 (11)	0.0032 (11)
O4	0.0294 (14)	0.0245 (14)	0.0270 (14)	−0.0045 (10)	0.0191 (12)	−0.0049 (11)
O3	0.0205 (12)	0.0112 (11)	0.0261 (13)	−0.0006 (9)	0.0162 (11)	0.0012 (10)
O6	0.0311 (14)	0.0253 (14)	0.0243 (14)	0.0014 (11)	0.0154 (12)	0.0038 (11)
O2	0.0255 (13)	0.0127 (12)	0.0439 (15)	−0.0017 (10)	0.0228 (12)	−0.0027 (11)
O7	0.0635 (19)	0.0265 (15)	0.0297 (15)	−0.0021 (14)	0.0275 (15)	0.0026 (12)
O5	0.0299 (14)	0.0218 (13)	0.0312 (14)	−0.0048 (11)	0.0158 (12)	−0.0053 (11)

C7	0.0202 (17)	0.0164 (17)	0.0204 (17)	0.0005 (13)	0.0139 (15)	0.0027 (14)
C2	0.0191 (17)	0.0157 (17)	0.0214 (17)	0.0006 (13)	0.0136 (15)	0.0012 (14)
C8	0.0174 (16)	0.0097 (16)	0.0256 (18)	0.0063 (13)	0.0135 (15)	0.0054 (14)
C9	0.0231 (18)	0.028 (2)	0.0270 (19)	−0.0079 (16)	0.0168 (17)	−0.0048 (17)
C1	0.0243 (19)	0.0166 (18)	0.0210 (19)	0.0015 (13)	0.0161 (16)	0.0041 (13)
C10	0.049 (3)	0.037 (2)	0.023 (2)	−0.0107 (19)	0.017 (2)	−0.0014 (18)
C6	0.029 (2)	0.0200 (18)	0.041 (2)	0.0016 (16)	0.0257 (18)	0.0003 (17)
C3	0.0239 (18)	0.0208 (18)	0.0279 (19)	−0.0018 (15)	0.0149 (16)	0.0013 (16)
C4	0.0168 (18)	0.033 (2)	0.035 (2)	−0.0030 (16)	0.0143 (17)	0.0025 (18)
C5	0.0228 (19)	0.027 (2)	0.044 (2)	0.0075 (15)	0.0213 (18)	0.0055 (18)

Geometric parameters (Å, º)

Eu1—O1^{i}	2.570 (2)	Eu1—O4^{ii}	2.605 (2)
Eu1—O1	2.397 (2)	Eu1—O5	2.352 (2)
Eu1—O2^{i}	2.474 (2)	Eu1—O6^{i}	2.434 (3)
Eu1—O3	2.381 (2)	Eu1—O7	2.446 (2)
Eu1—O3^{ii}	2.484 (2)		
O1—Eu1—Eu1^{i}	100.62 (6)	Eu1—O3—Eu1^{i}	107.20 (8)
O1^{i}—Eu1—Eu1^{i}	36.44 (5)	C8—O3—Eu1^{i}	95.16 (19)
O1—Eu1—O1^{i}	135.94 (6)	C8—O3—Eu1	126.05 (19)
O1—Eu1—O4^{ii}	112.11 (8)	C9—O6—Eu1^{ii}	133.7 (2)
O1^{i}—Eu1—O4^{ii}	110.21 (7)	C1—O2—Eu1^{ii}	96.9 (2)
O1—Eu1—O3^{ii}	72.40 (7)	Eu1—O7—H7A	121.4
O1—Eu1—O6^{i}	69.36 (8)	Eu1—O7—H7B	120.3
O1—Eu1—O2^{i}	138.23 (8)	H7A—O7—H7B	104.5
O1—Eu1—O7	132.57 (9)	C9—O5—Eu1	134.6 (2)
O4^{ii}—Eu1—Eu1^{i}	146.65 (5)	C2—C7—C8	126.3 (3)
O3—Eu1—Eu1^{i}	37.29 (5)	C6—C7—C2	119.2 (3)
O3^{ii}—Eu1—Eu1^{i}	141.16 (5)	C6—C7—C8	114.4 (3)
O3—Eu1—O1^{i}	71.11 (7)	C7—C2—C1	123.0 (3)
O3—Eu1—O1	72.28 (8)	C3—C2—C7	118.7 (3)
O3^{ii}—Eu1—O1^{i}	130.07 (7)	C3—C2—C1	118.3 (3)
O3^{ii}—Eu1—O4^{ii}	51.12 (7)	O4—C8—Eu1^{i}	63.93 (18)
O3—Eu1—O4^{ii}	162.55 (8)	O4—C8—O3	120.3 (3)
O3—Eu1—O3^{ii}	141.75 (4)	O4—C8—C7	119.7 (3)
O3—Eu1—O6^{i}	79.11 (8)	O3—C8—Eu1^{i}	58.54 (16)
O3—Eu1—O2^{i}	119.05 (7)	O3—C8—C7	119.3 (3)
O3—Eu1—O7	82.61 (9)	C7—C8—Eu1^{i}	156.5 (2)
O6^{i}—Eu1—Eu1^{i}	66.91 (5)	O6—C9—C10	119.2 (3)
O6^{i}—Eu1—O1^{i}	80.35 (8)	O5—C9—O6	124.1 (3)
O6^{i}—Eu1—O4^{ii}	118.34 (8)	O5—C9—C10	116.7 (3)
O6^{i}—Eu1—O3^{ii}	75.15 (8)	O1—C1—Eu1^{ii}	62.34 (16)
O6^{i}—Eu1—O2^{i}	73.70 (8)	O1—C1—C2	120.2 (3)
O6^{i}—Eu1—O7	144.26 (8)	O2—C1—Eu1^{ii}	57.86 (16)
O2^{i}—Eu1—Eu1^{i}	81.77 (5)	O2—C1—O1	120.1 (3)
O2^{i}—Eu1—O1^{i}	51.37 (7)	O2—C1—C2	119.6 (3)

O2^{i}—Eu1—O4^{ii}	69.76 (7)	C2—C1—Eu1^{ii}	174.1 (2)
O2^{i}—Eu1—O3^{ii}	79.99 (7)	C9—C10—H10A	109.5
O7—Eu1—Eu1^{i}	79.97 (7)	C9—C10—H10B	109.5
O7—Eu1—O1^{i}	64.69 (8)	C9—C10—H10C	109.5
O7—Eu1—O4^{ii}	82.51 (9)	H10A—C10—H10B	109.5
O7—Eu1—O3^{ii}	133.38 (9)	H10A—C10—H10C	109.5
O7—Eu1—O2^{i}	89.12 (9)	H10B—C10—H10C	109.5
O5—Eu1—Eu1^{i}	125.35 (6)	C7—C6—H6	119.5
O5—Eu1—O1	71.29 (8)	C5—C6—C7	120.9 (3)
O5—Eu1—O1^{i}	133.75 (8)	C5—C6—H6	119.5
O5—Eu1—O4^{ii}	73.60 (8)	C2—C3—H3	119.3
O5—Eu1—O3	92.82 (8)	C4—C3—C2	121.3 (3)
O5—Eu1—O3^{ii}	89.44 (7)	C4—C3—H3	119.3
O5—Eu1—O6^{i}	140.44 (9)	C3—C4—H4	120.1
O5—Eu1—O2^{i}	139.98 (8)	C5—C4—C3	119.8 (3)
O5—Eu1—O7	70.49 (9)	C5—C4—H4	120.1
Eu1—O1—Eu1^{ii}	104.00 (8)	C6—C5—H5	120.0
C1—O1—Eu1^{ii}	91.53 (18)	C4—C5—C6	119.9 (3)
C1—O1—Eu1	139.6 (2)	C4—C5—H5	120.0
C8—O4—Eu1^{i}	90.7 (2)		

Eu1—O1—C1—Eu1^{ii}	113.9 (3)	C7—C2—C3—C4	1.7 (5)
Eu1^{ii}—O1—C1—O2	−3.0 (3)	C7—C6—C5—C4	0.7 (6)
Eu1—O1—C1—O2	110.9 (3)	C2—C7—C8—Eu1^{i}	140.5 (5)
Eu1^{ii}—O1—C1—C2	174.0 (3)	C2—C7—C8—O4	−127.1 (3)
Eu1—O1—C1—C2	−72.1 (4)	C2—C7—C8—O3	62.7 (4)
Eu1^{i}—O4—C8—O3	16.5 (3)	C2—C7—C6—C5	−2.9 (5)
Eu1^{i}—O4—C8—C7	−153.6 (2)	C2—C3—C4—C5	−3.9 (5)
Eu1—O3—C8—Eu1^{i}	115.7 (2)	C8—C7—C2—C1	8.9 (5)
Eu1—O3—C8—O4	98.2 (3)	C8—C7—C2—C3	−174.4 (3)
Eu1^{i}—O3—C8—O4	−17.4 (3)	C8—C7—C6—C5	173.7 (3)
Eu1—O3—C8—C7	−91.6 (3)	C1—C2—C3—C4	178.4 (3)
Eu1^{i}—O3—C8—C7	152.8 (2)	C6—C7—C2—C1	−174.9 (3)
Eu1^{ii}—O6—C9—O5	21.5 (5)	C6—C7—C2—C3	1.7 (5)
Eu1^{ii}—O6—C9—C10	−158.7 (3)	C6—C7—C8—Eu1^{i}	−35.8 (7)
Eu1^{ii}—O2—C1—O1	3.1 (3)	C6—C7—C8—O4	56.7 (4)
Eu1^{ii}—O2—C1—C2	−173.9 (3)	C6—C7—C8—O3	−113.6 (3)
Eu1—O5—C9—O6	23.5 (5)	C3—C2—C1—O1	177.3 (3)
Eu1—O5—C9—C10	−156.3 (3)	C3—C2—C1—O2	−5.7 (5)
C7—C2—C1—O1	−6.1 (5)	C3—C4—C5—C6	2.7 (5)
C7—C2—C1—O2	170.9 (3)		

Symmetry codes: (i) −*x*+3/2, *y*+1/2, −*z*+3/2; (ii) −*x*+3/2, *y*−1/2, −*z*+3/2.

Hydrogen-bond geometry (Å, º)

D—H···*A*	*D*—H	H···*A*	*D*···*A*	*D*—H···*A*
O7—H7*A*···O4^{iii}	0.85	2.17	2.9384	149

O7—H7*B*···O6^{iv}	0.85	2.28	3.0438	150
C3—H3···O2	0.93	2.46	2.7741	100

Symmetry codes: (iii) x, $-y$, $z-1/2$; (iv) $-x+1/2$, $y+1/2$, $-z+1/2$.